The Astrophysical Journal Letters, 913:L2 (6pp), 2021 May 20 https://doi.org/10.3847/2041-8213/abfb74

Astromers in the Radioactive Decay of r-process Nuclei

G. Wendell Misch[1,2,3], T. M. Sprouse[1,2], and M. R. Mumpower[1,2,3]
[1] Theoretical Division, Los Alamos National Laboratory, Los Alamos, NM 87545, USA; wendell@lanl.gov
[2] Center for Theoretical Astrophysics, Los Alamos National Laboratory, Los Alamos, NM 87545, USA
[3] Joint Institute for Nuclear Astrophysics—Center for the Evolution of the Elements, USA
Received 2021 March 5; revised 2021 April 16; accepted 2021 April 24; published 2021 May 18

Abstract

Certain nuclear isomers are well known to affect nucleosynthesis with important observable consequences (e.g., ^{26}Al and ^{180}Ta). We study the impact of nuclear isomers in the context of rapid neutron capture process (*r*-process) nucleosynthesis. We demonstrate that nuclear isomers are dynamically populated in the *r* process and that some are populated far from thermal equilibrium; this makes them astrophysical isomers, or "astromers." We compute thermally mediated transition rates between long-lived isomers and the corresponding ground states in neutron-rich nuclei. We calculate the temperature-dependent β-decay feeding factors, which represent the fraction of material going to each of the isomer and ground state daughter species from the β-decay parent species. We simulate nucleosynthesis following the decay of a solar-like *r*-process composition and include as separate species nuclear excited states with measured terrestrial half-lives greater than 100 μs. We introduce a new metric to identify those astromers most likely to be influential and summarize them in a table. Notable entries include many second peak nuclei (e.g., the Te isotopic chain) and previously overlooked isomers in stable nuclei (e.g., ^{119}Sn, ^{131}Xe, and ^{195}Pt). Finally, we comment on the capacity of isomer production to alter radioactive heating in an *r*-process environment.

Unified Astronomy Thesaurus concepts: Nuclear astrophysics (1129); R-process (1324); Nuclear physics (2077)

1. Introduction

The existence of long-lived excited (metastable) states of atomic nuclei, known as nuclear isomers, was proposed by Soddy (1917) and verified by Hahn (1921) a century ago (Walker & Podolyák 2020). The study of nuclear isomers has since been a focus of experimental efforts throughout the chart of nuclides, often requiring challenging measurements (Raut et al. 2013; Simpson et al. 2014; Patel et al. 2014; Watanabe et al. 2014; Svirikhin et al. 2017; Andreev et al. 2019; Sikorsky et al. 2020). Over 700 nuclei have been identified as possessing isomeric states with half-lives greater than 100 μs (Brown et al. 2018). Theoretical nuclear structure methods (Brown & Rae 2014) are able to characterize some of these isomers, which can arise due to large spin differences (spin traps), differences in nuclear deformation (shape coexistence/shape isomers), and large differences in the projection of spin along the axis of symmetry in a deformed nucleus (*K* isomers; Dracoulis et al. 2016).

Despite the experimental and theoretical progress in terrestrial studies, much remains uncertain regarding the population of nuclear isomers in astrophysical environments (Aprahamian & Sun 2005; Hayakawa et al. 2005, 2009). The most well studied cases in nuclear astrophysics are in relatively light nuclei. For instance, ^{26}Al can be used as a tracer of star formation due to the long half-life of the ground state (Mahoney et al. 1982; Diehl et al. 1995), but its in situ production is complicated by a low-lying isomer (Gupta & Meyer 2001; Runkle et al. 2001; Banerjee et al. 2018). The production of ^{34}Cl may be observable immediately after a nova (Coc et al. 1999), while ^{85}Kr is a branch point in the slow neutron capture (*s*) process (Abia et al. 2001) with implications for cosmochronmetry (Ward 1977); both of these nuclei are influenced by isomers.

In stark contrast, while mechanisms for inclusion of these additional states in nucleosynthesis codes exist (Reifarth et al. 2018), the population of astrophysically metastable nuclear isomers (astromers) is a missing component in the simulation of *r*-process nucleosynthesis. Exploration of astromers should impact searches for the most influential nuclei to measure at radioactive beam facilities (Mumpower et al. 2016; Horowitz et al. 2019), and it overlaps with modern multimessenger astronomy (Abbott et al. 2017; Tanvir et al. 2017; Troja et al. 2017; Watson et al. 2019; Wang et al. 2020; Domoto et al. 2021).

In environments where the *r* process may operate, nuclear isomers can be populated thermally then frozen out as the temperature drops rapidly. They can also be fed by β-decay of more neutron-rich isotopes, as well as through other nuclear reactions such as neutron capture and fission (Wisshak et al. 2006; Okumura et al. 2018). The direct population of nuclear isomers has recently been shown to be potentially influential in the radioactive heating of *r*-process events by Fujimoto & Hashimoto (2020). They compared a no-isomer simulation against two that included several hand-picked isomers; both isomer models essentially replaced the ground state properties of the selected nuclei with the isomer properties.

In this work, we explore for the first time dynamical freeze-out as well as the thermal and β-decay population mechanisms of nuclear isomers in the *r* process. We demonstrate that a range of nuclear isomers are significantly populated in the *r* process between first peak (mass number, $A \sim 80$) and third peak ($A \sim 195$) elements. We introduce an astromer importance rating (AIR) to identify prominent astromers among our included isomers, and we show the effects of our detailed treatment of known nuclear isomers on an *r*-process heating curve. By dynamically including both nuclear isomers and their corresponding ground states (GS), we account for a previously unaddressed nonequilibrium process in simulations of heavy element nucleosynthesis.

2. Nuclear Isomers and Nucleosynthesis

2.1. Isomer Treatment

We treat isomers with half-lives greater than 100 μs and GS as distinct "long-lived" species. We use the method of

Misch et al. (2020) to calculate the thermal-photon-bath mediated transition rates between long-lived states via intermediate states: we explicitly calculate thermally mediated transition probabilities between every pair of nuclear levels (cf. Hayakawa et al. 2010), then implicitly solve for the total transition rate through all possible pathways between the isomer and GS. This approach does not rely on approximations to solve the linear system of equations (cf. Gupta & Meyer 2001), and it allows a consistent treatment of the GS and isomers at all temperatures that can be directly incorporated into nucleosynthesis calculations. We compute the temperature-dependent β-decay rates of long-lived states using the ensemble formalism of Gupta & Meyer (2001).

To account for the feeding of β-decay daughter nuclei with isomers, we combine laboratory β-decay $\log(ft)$ values to specific daughter states with that state's probability to contribute to each daughter ensemble; we use available laboratory β-decay rates and measured β intensities to obtain the β feeding when $\log(ft)$ values are unavailable. This yields temperature-dependent decay rates into each of the daughter "species." When β intensities are unavailable in the literature, we assume that all decays go to the daughter ground state.

Our isomer calculations use experimental level energies, half-lives, spin-parity assignments, γ intensities, and $\log(ft)$ values/β intensities from ENSDF.[4] We include all experimental levels if there are fewer than 30 reported; if there are more than 30 levels, we include all levels up to the 10 levels above the highest-lying isomer (minimum 30); the analysis of Coc et al. (1999) shows that this selection is more than adequate to accurately compute transition rates. For unmeasured γ transitions, we use the Weisskopf approximation (Weisskopf & Wigner 1930).

2.2. Nucleosynthesis

We simulate nucleosynthesis with the Jade nuclear reaction network of Sprouse et al. (2021). Jade uses a matrix exponential solver that enables the inclusion of temperature-dependent effects on nuclear transmutation rates. This allows us to track the population and depopulation of the long-lived states of individual isotopes as a function of time. Our network explicitly includes all isomeric states of each isotope, but for clarity, our arguments are presented as though each isotope has at most one isomer. For nuclei with isomers, we use the treatment in Section 2.1. Otherwise, we take laboratory ground-state half-lives from evaluated data[5] (Brown et al. 2018; Audi et al. 2017) and supplement with theoretical predictions for yet-to-be-measured nuclei (Möller et al. 2019).

To investigate a wide mass range of isomer production in a site-independent way, we place a solar-like distribution of r-process material (Arnould et al. 2007) between mass numbers $A = 69$ to $A = 212$ far from stability; the composition consists of all three major r-process abundance peaks. We focus on the population of nuclear isomers after ~15 minutes. In this epoch, all relevant neutron captures have finished, and β-decay, thermally induced excitation, and radiative/thermally stimulated de-excitation are the primary nuclear reaction channels. Temperature will therefore have become the only relevant environmental quantity, and the isotopic abundances will have converged to an isochrone (Sprouse et al. 2021). We report our results using the wind-like ejecta of Zhu et al. (2018), which is based on a homologous expansion into free space (Lippuner & Roberts 2015). We have studied a variety of other trajectories and found qualitatively similar results. We stop our calculations after ~3600 days (10 yr).

3. AIR: Astromer Importance Rating

We define the population ratio $R_{i,m}$ of the isomer species of isotope i as

$$R_{i,m} = \frac{Y_{i,m}}{\sum_j Y_{i,j}}. \quad (1)$$

The abundance $Y_{i,j}$ is the number of isotope i in state j per baryon of material. Thus $R_{i,m}$ is the ratio of the isomer abundance to the total abundance of the isotope. For the sake of brevity and legibility, we suppress the indices on R from here on.

By finding the maximum value of R over time for each isomer, we can identify which are populated in a nucleosynthesis event. Figure 1 shows this value for the 96 isotopes which at some time in our simulation had $R \geqslant 0.1$. Many of the most populated isomers lie in one of the three r-process abundance peaks located at $A \sim 80$, $A \sim 130$, and $A \sim 195$. The isomers in these three peaks may be especially significant to the r process, as they not only represent a significant fraction of their respective isotopes, but also these isotopes are among the most abundantly populated during an r-process event.

However, not all highly populated isomers are astromers. They may not freeze-out before the isotope has decayed away, or they may not decay at a rate appreciably different from the ground state. And even if an isomer is an astromer, the isotope may not be sufficiently abundant to influence quantities such heating, decay lines, and isotopic abundances (we use the nonspecific term "evolution" to refer to the change of all such quantities with time). Therefore, we develop a metric to assist in identifying important astromers.

A species affects evolution through its destruction (decay or de-excitation). For example, consider an abundant ground state of a stable isotope in a cold environment. This species does not participate in the evolution since it neither affects heating nor drives change in abundance. Similarly, a rapidly decaying isotope will not affect the environment if its abundance is very low. We calculate the specific activity a of each species to measure its influence.

$$a_{i,j} = \lambda_{i,j} Y_{i,j} \quad (2)$$

$$\lambda_{i,j} \equiv \sum_{\text{channels}} \lambda_{i,j}^{\text{channel}}. \quad (3)$$

The λs are destruction rates (s^{-1}), and the indices i and j are as in Equation (1); we will suppress the a indices i and j going forward, taking j to always be the isomer. In this work, our channels consist exclusively of β decays and thermally mediated internal transitions. Activity then quantifies the number of actions taken by an isotope (transitions and/or decays) per baryon of material per second. The most active isotopes at a given time drive the evolution, provided that their activity is not simply internal transitions back and forth between the ground state and isomer. This brings us to the thermally weighted abundance imbalance.

[4] From ENSDF database as of 2020 June 29. Version available at http://www.nndc.bnl.gov/ensarchivals/.

[5] https://www-nds.iaea.org/public/download-endf/ENDF-B-VIII.0/

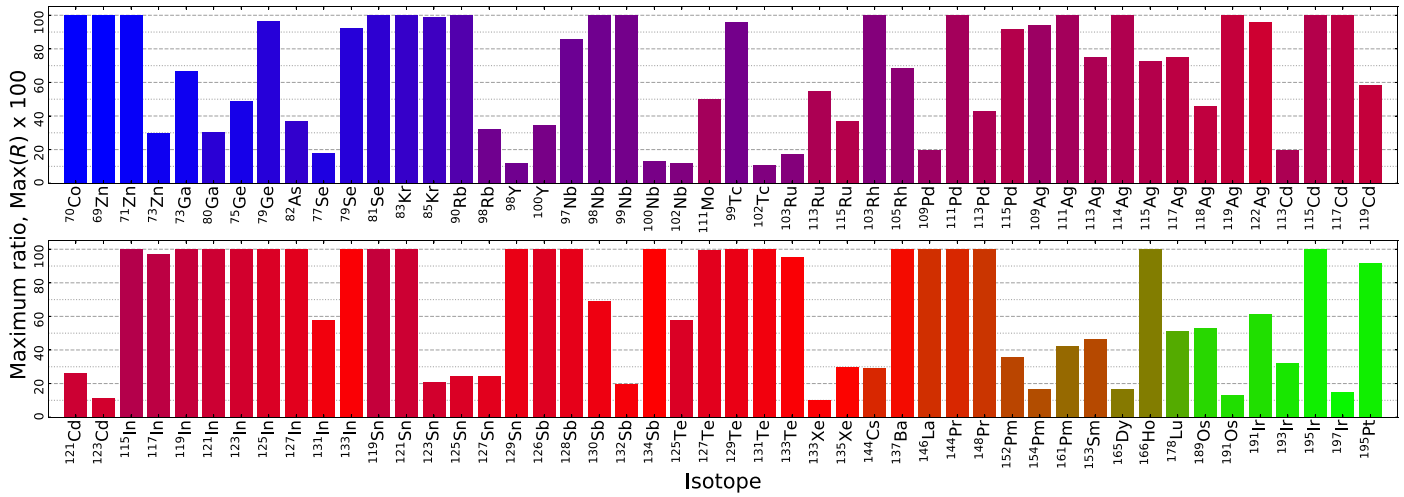

Figure 1. The maximum isomer population ratio, Max(R) $\times$ 100, over the course of our simulation for isomers populated above 10%. Color indicates approximately the r-process abundance peak the nucleus resides in; see Figure 2.

To be an astromer, we also require that the isomer m be out of thermal equilibrium with the ground state g; otherwise, its isomeric quality does not meaningfully impact the evolution as nucleosynthesis proceeds (compared to assuming thermal equilibrium level populations). To assess how far the populations are from thermal equilibrium, we first define a thermally scaled abundance $\widetilde{Y}$ that enables us to compare the GS and isomer abundances on equal footing.

$$\widetilde{Y} \equiv \frac{Y}{(2J+1)e^{-E/T}}. \tag{4}$$

In thermal equilibrium, $\widetilde{Y}_g = \widetilde{Y}_m$. Now, to quantify how far these values are from equality, we use (the absolute value of) their imbalance I.

$$I(\widetilde{Y}_g, \widetilde{Y}_m) = \frac{|\widetilde{Y}_g - \widetilde{Y}_m|}{\widetilde{Y}_g + \widetilde{Y}_m}. \tag{5}$$

If the scaled abundances are equal (in thermal equilibrium), the imbalance is zero, and as they diverge, the imbalance tends toward unity. Imbalance has the helpful feature of being independent of the scale of the abundances without going to infinity the way a ratio of the two quantities might; this second point is important when, e.g., only one state is populated. Furthermore, unlike a ratio, the imbalance will be "large" (near unity) for inputs that are very different from one another regardless of which is greater.

Taken as a product, the activity a, imbalance I, and population ratio R give a useful metric—the AIR—to help identify populated and influential astromers.

$$\begin{aligned} \text{AIR} &= \text{Activity} \times \text{Imbalance} \times \text{population Ratio} \\ &= a \times I \times R. \end{aligned} \tag{6}$$

AIR selects isomers that (1) have high activity, (2) are far from thermal equilibrium, and (3) have a significant population relative to ground. These are the necessary ingredients for an influential astromer. Note that it is possible for a slow-decaying astromer to effectively reduce a. However, at later times, everything with a high a will have decayed away, leaving the slower astromer to dominate the AIR then. We therefore search AIR over a broad range of times to maximize our ability to find important astromers.

4. Results

We computed the AIR for every nuclear isotope in our simulation to isolate influential astromers. Figure 2 shows the AIR for the 25 isotopes which, at some simulation timestep, are among the top five most important astromers as ranked by AIR.

Figure 2 shows that the most dominant first peak astromers (blue) are relevant for about 1 day. A surprising contender on this timescale is ^{85}Kr, which is most famous as an s-process branch point. In the r-process, it has the highest AIR from $\sim$0.5 to 1 day due to the $>90\%$ feeding of the isomer by ^{85}Br. This greatly accelerates the decay to ^{85}Rb, and it may produce an electromagnetic signal.

In contrast with the first peak astromers, those located in the second peak (red) persist over much of our simulation, ranging from 0.01 to 10,000 days. As a result, they have the potential to affect many aspects of the evolution throughout a range of observational timescales. At the earliest times in our simulation, around 0.01 days, we note the formation and large AIR of ^{128,130}Sb and ^{131}Te, which contribute alongside a number of additional isomers located in the first and third peaks. By 30 days, all remaining isomers are located among the second peak nuclei, the most notable of which include ^{125,127}Te. Finally, we identify the particularly interesting isomer in ^{129}Te. It remains important across all epochs of our simulation, from 0.01 days to 1 year, reflecting a complex interplay between the β-decay feeding parent, thermal excitation, and de-excitation.

We identify ^{195}Pt as the dominant astromer located in the third r-process peak (green). In contrast with the conventional assumption that this isotope is stable upon population via the ground state β decay of ^{195}Ir, our calculations show that the isomer of ^{195}Pt may be populated directly from the β decay of the isomer of ^{195}Ir. The ^{195}Pt isomer de-excites on a timescale of $\sim$4 days, which is relevant to the study of electromagnetic signals associated with the r process.

In the interest of readability, Figure 2 shows only those astromers that rank in the top five by AIR. When we expand our enumeration of r-process astromers to include the top 10, we identify only 11 additional astromers. This highlights the effectiveness of AIR as a filter for distinguishing astromers

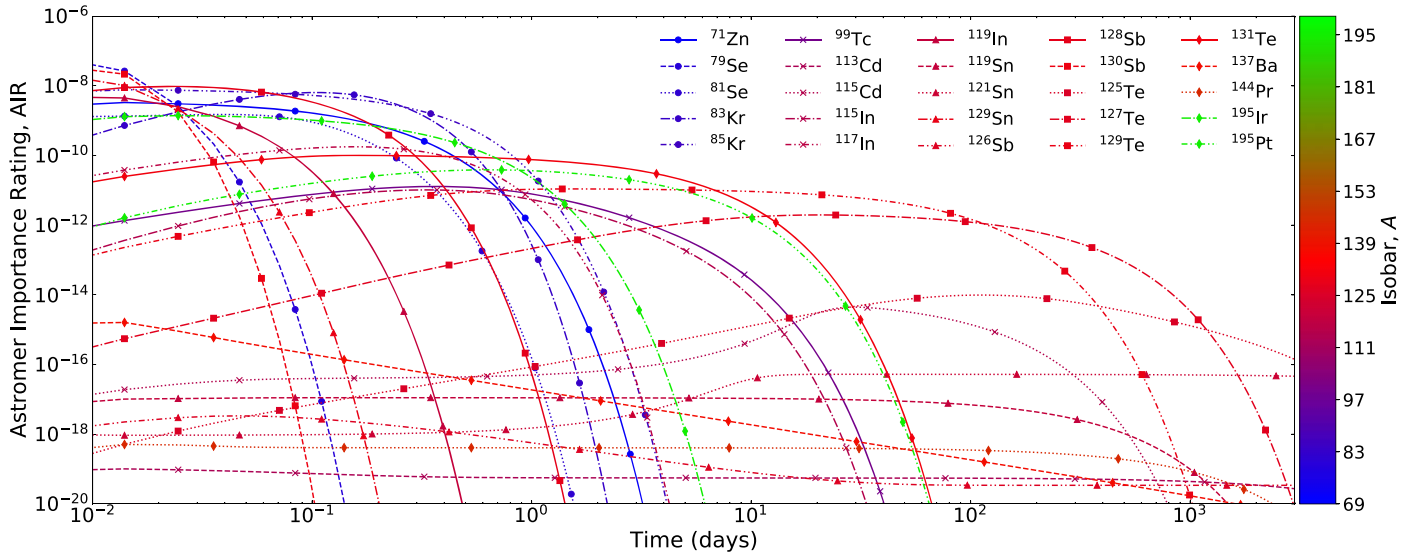

Figure 2. Influential *r*-process astromers ranked by their AIR. We show isotopes with AIR values that appear among the top five at some point in our simulation. Color indicates approximately the *r*-process abundance peak the nucleus resides in: first (blue), second (red), or third (green).

from the broader population of isomers: the list of isomers identified as influential astromers is relatively insensitive to the particular choice of AIR top-*N*. We summarize our expanded (top 10) list of astromers in Table 1.

Notably, there are three species in Table 1 that do not appear in Figure 1: ^{93,95}Nb and ^{131}Xe. This is because while the isomers might not be heavily populated relative to the ground state (low *R*), they have comparatively high activities *a* and large thermal population imbalances *I*.

The astromers identified in Table 1 that change β-decay rates will affect *r*-process heating. Some (e.g., ^{115}Cd, ^{127,129,131}Te) will defer heating by delaying decay, while others (e.g., ^{85}Kr, ^{128,130}Sb) partially counteract this trend by accelerating decay.

Furthermore, astromers may generate identifiable *x*-ray or γ-ray signals either directly through de-excitation (^{85}Kr, ^{115}In, ^{119}Sn, ^{131,133}Xe, and ^{195}Pt) or indirectly subsequent to β decay (any with $T_{1/2} \gtrsim 1$ day). Such isomers could be used to associate future *r*-process observations with the production of specific nuclei.

We emphasize two points about the relationship between available nuclear data and our astromer calculations. First, more complete excited state data would improve our ground state $\leftrightarrow$isomer transition rates. Specifically, measurements of intermediate state half-lives and γ intensities enable more reliable calculations of thermally mediated transition rates. This is exemplified by ^{128}Sb, whose isomer dramatically accelerates the decay of the $A = 128$ mass chain. All excited states of this nucleus reported in ENSDF connect to the isomer—which itself has an unknown energy—and the missing links to ground suppress our calculated transition rate.

Second, we need more complete β intensities to compute reliable feeding factors. Because we assume that decays with unpublished intensities always go to ground in the daughter, we preclude the possibility that such decays populate a daughter isomer. The production of ^{170}Ho is one example of this issue: the β intensities of ^{170}Dy are unknown, leading to our inability to effectively calculate the feeding factors into the ^{170}Ho isomer (Misch et al. 2020). The $A = 115$ and $A = 129$ mass chains are particularly striking examples of missing β-decay information. While the feeding factors from the ^{115}Cd and ^{129}Sn parents are measured, we lack data on how multiple earlier ancestors populate isomers in those parents. Experimental and theoretical efforts to quantify unknown β intensities would improve understanding of the population of astromers in *r*-process events.

One of the key roles that isomers have recently been proposed to play is in adjusting the timescale on which nuclear energy is released during the radioactive decay toward stability immediately following *r*-process nucleosynthesis (Fujimoto & Hashimoto 2020). To investigate these effects, we performed calculations for the radioactive heating of *r*-process material both with and without the consideration of isomers. We show our calculations of these two heating rates as a function of time in Figure 3.

Within the first day, some astromers effectively store energy by slowing radioactive decay toward stability as a result of their comparatively longer half-lives. On longer timescales (10–100 days), the slower decay of these astromers leads to a gradual release of the energy they had previously retained, with the effect of boosting the heating by about 25%. Analogous cycles of energy retention and release by astromers tend to repeat on longer timescales, the next of which begins around 200 days. We find the inclusion of temperature-dependent β-decay rates, as well as thermally induced excitation and spontaneous/thermally stimulated de-excitation between long-lived nuclear states, tempers the dramatic effects suggested by Fujimoto & Hashimoto (2020).

5. Conclusions

We have demonstrated for the first time the dynamic population of nuclear isomers in the *r* process. We have identified astrophysical isomers (astromers) which may be influential in a number of distinct ways.

The astromer in ^{71}Zn delays heating from $A = 71$ decay to the few-hour timescale, while ^{85}Kr and ^{128}Sb accelerate their respective decay chains to a similar timescale. Thus, alterations to the heating curve may arise from simultaneous delay and acceleration of decay in different isotopes. Second-peak astromers (especially in Te isotopes) are likely the most influential from $\sim$1 day to at least 10 yr; they may affect late-time heating and/or produce observable decay lines. Surprisingly, even isomers in stable isotopes (e.g., ^{119}Sn, ^{131}Xe, and ^{195}Pt) may be populated

Table 1
Astromer Importance Rating (AIR) Top 10 Selected at Each Time Point $t \gtrsim 15$ Minutes

Isotope	E_m (keV)	J^π_g	J^π_m	$T_{1/2\ g}$ (s)	$T_{1/2\ m}$ (s)	$B_{m\beta}$ (%)	$T_{\rm pop}$	Notes
^{69}Zn	438.636	$1/2^-$	$9/2^+$	3.38×10^3	4.95×10^4	0.033	3 minutes	λ^β slowed for 14 hours, EM signal[a]
^{71}Zn	157.7	$1/2^-$	$9/2^+$	1.47×10^2	1.43×10^4	100	20 s	λ^β slowed for 4 hours
^{79}Se	95.77	$7/2^+$	$1/2^-$	1.03×10^{13}	2.35×10^2	0.056	9 minutes	$T_{1/2\ m} < T_{\rm pop}$, no new effect
^{81}Se	103.00	$1/2^-$	$7/2^+$	1.11×10^3	3.44×10^3	0.051	30 s	λ^β slowed for 1 hour
^{83}Kr	41.5575	$9/2^+$	$1/2^-$	stable	6.59×10^3	0	2.5 hr	γ only, likely no effect
^{85}Kr	304.871	$9/2^+$	$1/2^-$	3.39×10^8	1.61×10^4	78.8	3 minutes	λ^β accelerated for 5 hr[b], EM signal[a]
^{93}Nb	30.77	$9/2^+$	$1/2^-$	stable	5.09×10^8	0	1.6 Myr	$T_{1/2} < T_{\rm pop}$, no new effect
^{95}Nb	235.69	$9/2^+$	$1/2^-$	3.02×10^6	3.12×10^5	5.6	64 days	$T_{1/2} < T_{\rm pop}$, no new effect
^{97}Nb	743.35	$9/2^+$	$1/2^-$	4.33×10^3	5.87×10^1	0	17 hr	$T_{1/2} < T_{\rm pop}$, no new effect
^{99}Tc	142.684	$9/2^+$	$1/2^-$	6.66×10^{12}	2.16×10^4	0.0037	66 hr	$T_{1/2\ m} < T_{\rm pop}$,no new effect
^{113}Cd	263.54	$1/2^+$	$11/2^-$	2.54×10^{23}	4.45×10^8	99.86	6 hr	low Y_m,long $T_{1/2}$,likely unobservable
^{115}Cd	181.0	$1/2^+$	$(11/2)^-$	1.92×10^5	3.85×10^6	100	20 minutes	λ^β slowed for 45 days
^{117}Cd	136.4	$1/2^+$	$(11/2)^-$	8.96×10^3	1.21×10^4	100	70 s	λ^β slowed for 3.4 hr
^{115}In	336.244	$9/2^+$	$1/2^-$	1.39×10^{22}	1.61×10^4	5.0	54 hr	^{115}Sn production boosted,EM signal[a]
^{117}In	315.303	$9/2^+$	$1/2^-$	2.59×10^3	6.97×10^3	52.9	3 hr	$T_{1/2} < T_{\rm pop}$,no new effect
^{119}In	311.37	$9/2^+$	$1/2^-$	1.44×10^2	1.08×10^3	95.6	3 minutes	λ^β slowed for 18 minutes
^{119}Sn	89.531	$1/2^+$	$11/2^-$	stable	2.53×10^7	0	3-18 minutes	EM signal[a]
^{121}Sn	6.31	$3/2^+$	$11/2^-$	9.73×10^4	1.39×10^9	22.4	4 minutes	λ^β slowed for 44 yr, EM signal[a]
^{129}Sn	35.15	$3/2^+$	$11/2^-$	1.34×10^2	4.14×10^2	100	1 s	λ^β slowed for 7 minutes
^{126}Sb	17.7	(8^-)	(5^+)	1.07×10^6	1.15×10^3	86	230 kyr	$T_{1/2} < T_{\rm pop}$, no new effect
^{128}Sb	0.0+X	8^-	5^+	3.26×10^4	6.25×10^2	96.4	1 hr	λ^β accelerated to 11 minutes $T_{1/2}$[b]
^{130}Sb	4.8	(8^-)	$(4, 5)^+$	2.37×10^3	3.78×10^2	100	4 minutes	λ^β accelerated to 6.3 minutes $T_{1/2}$[b]
^{125}Te	144.775	$1/2^+$	$11/2^-$	stable	4.96×10^6	0	3 yr	$T_{1/2\ m} < T_{\rm pop}$, no new effect
^{127}Te	88.23	$3/2^+$	$11/2^-$	3.37×10^4	9.17×10^6	2.4	4 days	λ^β slowed for 100 days, EM signal[a]
^{129}Te	105.51	$3/2^+$	$11/2^-$	4.18×10^3	2.9×10^6	36	4.5 hr	λ^β slowed for 34 days, EM signal[a]
^{131}Te	182.258	$3/2^+$	$11/2^-$	1.5×10^3	1.2×10^5	74.1	23 minutes	λ^β slowed for 33 hr, EM signal[a]
^{133}Te	334.26	$(3/2^+)$	$(11/2^-)$	7.5×10^2	3.32×10^3	83.5	2.5 minutes	λ^β slowed for 1 hr
^{131}Xe	163.930	$3/2^+$	$11/2^-$	stable	1.02×10^6	0	8 days	EM signal[a]
^{133}Xe	233.221	$3/2^+$	$11/2^-$	4.53×10^5	1.9×10^5	0	21 hr	EM signal[a]
^{137}Ba	661.659	$3/2^+$	$11/2^-$	stable	1.53×10^2	0	30 yr	$T_{1/2} < T_{\rm pop}$, no new effect
^{144}Pr	59.03	0^-	3^-	1.04×10^3	4.32×10^2	0.07	285 days	$T_{1/2} < T_{\rm pop}$, no new effect
^{166}Ho	5.969	0^-	7^-	9.66×10^4	3.79×10^{10}	100	82 hr	λ^β slowed for 1200 y
^{189}Os	30.82	$3/2^-$	$9/2^-$	stable	2.09×10^4	0	1 days	$T_{1/2} < T_{\rm pop}$, no new effect
^{191}Ir	171.29	$3/2^+$	$11/2^-$	stable	4.90×10^0	0	16 days	$T_{1/2\ m} < T_{\rm pop}$, no new effect
^{195}Ir	100	$3/2^+$	$11/2^-$	8.24×10^3	1.32×10^4	95	7 minutes	feeds ^{195}Pt isomer[c]
^{195}Pt	259.077	$1/2^-$	$13/2^+$	stable	3.46×10^5	0	4 hr	EM signal[a]

Notes. We use g and m to indicate the ground state and isomer, respectively. The isomer energy is E_m, and the J^π are the spin and parity of the respective levels (parentheses denote uncertain J^π). The half-lives ($T_{1/2}$) and β-decay branching for the isomer ($B_{m\beta}$) are as measured in the laboratory; $B_{m\beta}$ is the percent of isomer decays, which are β decays rather than internal transitions to another nuclear state. $T_{\rm pop}$ is the approximate timescale on which the isotope is populated, and the Notes column gives some brief comments on the nucleus.

[a] EM signals (detectable x-rays and γ-rays) are possible, but we do not study them carefully here.

[b] Nearly all parent β decay feeds the isomer, effectively bypassing the longer-lived ground state.

[c] To explore the ^{195}Pt isomer population, we assume all ^{195}Os β decay feeds the ^{195}Ir isomer (actual feeding unknown).

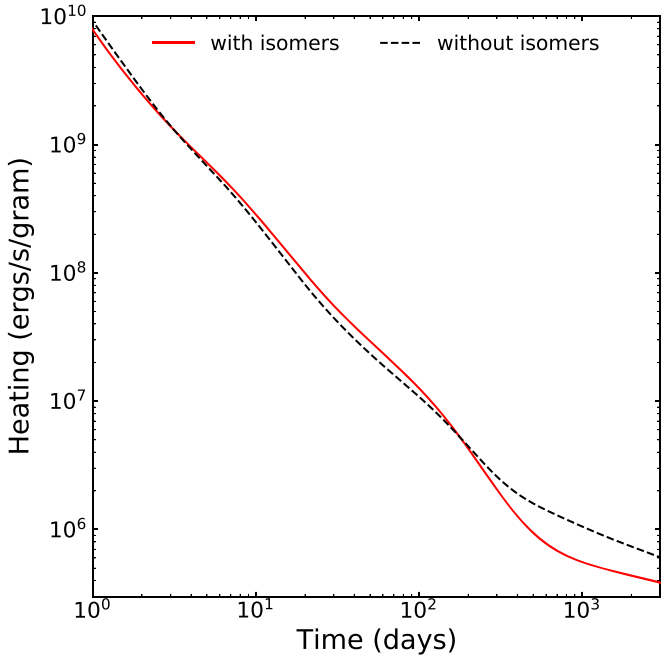

Figure 3. Radioactive heating from β-decay with and without isomers in an *r*-process event that includes all three major peaks. We find a 25% increase in heating from the inclusion of isomers between 3 and 100 days.

and observable. On still longer timescales, the astromers ^{121}Sn ($T_{1/2} = 44$ yr) and ^{166}Ho ($T_{1/2} = 1200$ yr) may play a role in galactic archeology.

Our work highlights the need for careful treatment of isomeric states when simulating the many and varied aspects of nucleosynthesis. This will be especially true when attempting to incorporate astromers that may originate from fission deposition or be dynamically produced and/or destroyed at early times when neutron capture is still active.

Current (Zhang et al. 2019; Nesterenko et al. 2020; Orford et al. 2020; Walker et al. 2020) and future studies at radioactive beam facilities that focus on elucidating the properties of nuclear isomers will help to refine our astromer predictions and strengthen our understanding of the creation of the heavy elements. This work provides fresh motivation for experimental campaigns to measure the beyond-ground-state properties—such as excited state half-lives and γ-ray intensities—that astromer evolution relies on.

We thank A. Couture, C. Fryer, B. Meyer, and F. Timmes for valuable discussions. G.W.M., T.M.S., and M.R.M. were supported by the US Department of Energy through the Los Alamos National Laboratory (LANL). LANL is operated by Triad National Security, LLC, for the National Nuclear Security Administration of the U.S. Department of Energy (contract No. 89233218CNA000001). G.W.M and M.R.M. were partly supported by the Laboratory Directed Research and Development program of LANL under project number 20190021DR. T.M.S. was partly supported by the Fission In R-process Elements (FIRE) Topical Collaboration in Nuclear Theory, funded by the U.S. Department of Energy.

ORCID iDs

G. Wendell Misch https://orcid.org/0000-0002-0637-0753
T. M. Sprouse https://orcid.org/0000-0002-4375-4369
M. R. Mumpower https://orcid.org/0000-0002-9950-9688

References

Abbott, B. P., Abbott, R., Abbott, T. D., et al. 2017, ApJL, 848, L12
Abia, C., Busso, M., Gallino, R., et al. 2001, ApJ, 559, 1117
Andreev, A. V., Savel'ev, A. B., Stremoukhov, S. Y., & Shoutova, O. A. 2019, PhRvA, 99, 013422
Aprahamian, A., & Sun, Y. 2005, NatPh, 1, 81
Arnould, M., Goriely, S., & Takahashi, K. 2007, PhR, 450, 97
Audi, G., Kondev, F. G., Wang, M., Huang, W. J., & Naimi, S. 2017, ChPhC, 41, 030001
Banerjee, P., Misch, G. W., Ghorui, S. K., & Sun, Y. 2018, PhRvC, 97, 065807
Brown, B., & Rae, W. 2014, NDS, 120, 115
Brown, D., Chadwick, M., Capote, R., et al. 2018, NDS, 148, 1
Coc, A., Porquet, M.-G., & Nowacki, F. 1999, PhRvC, 61, 015801
Diehl, R., Dupraz, C., Bennett, K., et al. 1995, A&A, 298, 445
Domoto, N., Tanaka, M., Wanajo, S., & Kawaguchi, K. 2021, arXiv:2103.15284
Dracoulis, G. D., Walker, P. M., & Kondev, F. G. 2016, RPPh, 79076301
Fujimoto, S.-i., & Hashimoto, M.-a 2020, MNRAS, 493, L103
Gupta, S. S., & Meyer, B. S. 2001, PhRvC, 64, 025805
Hahn, O. 1921, NW, 9, 84
Hayakawa, T., Kajino, T., Chiba, S., & Mathews, G. 2010, PhRvC, 81, 052801
Hayakawa, T., Shizuma, T., Chiba, S., et al. 2009, ApJ, 707, 859
Hayakawa, T., Shizuma, T., Kajino, T., et al. 2005, ApJ, 628, 533
Horowitz, C. J., Arcones, A., Côté, B., et al. 2019, JPhG, 46, 083001
Lippuner, J., & Roberts, L. F. 2015, ApJ, 815, 82
Mahoney, W. A., Ling, J. C., Jacobson, A. S., & Lingenfelter, R. E. 1982, ApJ, 262, 742
Misch, G. W., Ghorui, S. K., Banerjee, P., Sun, Y., & Mumpower, M. R. 2020, ApJS, 252, 2
Möller, P., Mumpower, M. R., Kawano, T., & Myers, W. D. 2019, ADNDT, 125, 1
Mumpower, M. R., Surman, R., McLaughlin, G. C., & Aprahamian, A. 2016, PrPNP, 86, 86
Nesterenko, D. A., Kankainen, A., Kostensalo, J., et al. 2020, PhLB, 808, 135642
Okumura, S., Kawano, T., Jaffke, P., Talou, P., & Chiba, S. 2018, Journal of Nuclear Science and Technology, 55, 1009
Orford, R., Kondev, F. G., Savard, G., et al. 2020, PhRvC, 102, 011303
Patel, Z., Söderström, P.-A., Podolyák, Z., et al. 2014, PhRvL, 113, 262502
Raut, R., Tonchev, A. P., Rusev, G., et al. 2013, PhRvL, 111, 112501
Reifarth, R., Fiebiger, S., Göbel, K., et al. 2018, IJMPA, 33, 1843011
Runkle, R., Champagne, A., & Engel, J. 2001, ApJ, 556, 970
Sikorsky, T., Geist, J., Hengstler, D., et al. 2020, PhRvL, 125, 142503
Simpson, G. S., Gey, G., Jungclaus, A., et al. 2014, PhRvL, 113, 132502
Soddy, F. 1917, SciMo, 5, 451
Sprouse, T. M., Misch, G. W., & Mumpower, M. R. 2021, arXiv:2102.03846
Svirikhin, A. I., Andreev, A. V., Yeremin, A. V., et al. 2017, PPNL, 14, 571
Tanvir, N. R., Levan, A. J., González-Fernández, C., et al. 2017, ApJL, 848, L27
Troja, E., Piro, L., van Eerten, H., et al. 2017, Natur, 551, 71
Walker, P., Hirayama, Y., Lane, G., et al. 2020, PhRvL, 125, 192505
Walker, P., & Podolyák, Z. 2020, PhyS, 95, 044004
Wang, X., N3AS Collaboration, N3AS Collaboration, Vassh, N., et al. 2020, ApJL, 903, L3
Ward, R. A. 1977, ApJ, 216, 540
Watanabe, H., Lorusso, G., Nishimura, S., et al. 2014, PhRvL, 113, 042502
Watson, D., Hansen, C. J., Selsing, J., et al. 2019, Natur, 574, 497
Weisskopf, V., & Wigner, E. P. 1930, ZPhy, 63, 54
Wisshak, K., Voss, F., Käppeler, F., et al. 2006, PhRvC, 73, 045807
Zhang, G., Watanabe, H., Dracoulis, G., et al. 2019, PhLB, 799, 135036
Zhu, Y., Wollaeger, R. T., Vassh, N., et al. 2018, ApJL, 863, L23